# Synthesis and characterization of non-equilibrium Ag-Ni nanowires: effect of electrodeposition parameters on the microstructure

R.K. Rai[1*], C. Srivastava[2]

[1]Malaviya National Institute of Technology Jaipur, Rajasthan-302017, India
[2]Indian Institute of Science, Bangalore-560012, India

Corresponding author: rajeshrai.bits@yahoo.in

## Abstract

The Ag-Ni system has drawn significant attention in recent past owing to its potential photonic, electronic, and magnetic applications. It is worth noting that the equilibrium phase diagram of the Ag-Ni system exhibits extremely wide immiscibility owing to a significant difference in Ag and Ni atomic sizes (~15%) and high positive enthalpy of mixing (~23%). In this study, Ag-Ni nanowires were prepared by adopting electrodeposition technique. Nanowire morphology was achieved using an anodisc having pores of ~200nm diameter. The present study provides a detailed compositional and microstructural characterization of different phases and microstructures in the Ag-Ni nanowires synthesized from adopting different electrodeposition conditions concerning deposition time, deposition current, and nanowire composition.

## 1. Introduction

For devise applications, isolated nano-sized solids provide two necessary incentives: (a) realization of unique microstructures and (b) realization of unique three-dimensional morphologies. It should, however, be noted that the above two "incentives" are strongly interdependent because of size and shape-sensitive phase stability within the nanoscale regimen. Designing solids at the nanoscale level thus requires optimization of the synthesis process to obtain a specific combination of size morphology and microstructure required for deriving particular functionalities. Due to their potential technological applications, single and multi-component nanowires have gained attention among isolated nano-sized solids [1], [2]. The microstructure and the physical properties of nanowires can be easily tuned by altering the aspect ratio of the nanowires. The change in physical properties with nanowire diameter can be emergent or monotonically varying in character[3].

Investigations of nano-sized solids have revealed unique size-dependent structures and microstructures that cannot be realized in bulk systems with similar compositions and environments[4], [5]. Fundamentally, phase stability at the nanoscale is guided by the same free energy minimization criterion as valid for the bulk case[6], [7]. However, the difference(s) in microstructure arises primarily due to the enormous energetic contribution from the specific surfaces and heterophase interfaces in the nano-size systems compared to the bulk systems. Furthermore, within the nanoscale regimen, the relative energetic contribution from specific surfaces and interfaces changes radically with minor changes in size[8], [9]. One exciting example is the increase in the propensity for solid solubility between immiscible component atoms confined in nano-sized volumes [8]. Bulk immiscibility is primarily due to a high positive enthalpy of mixing and strain effects arising from a significant difference in component atom sizes. This phenomenon is termed as the 'Miscibility Gap'[10]. The miscibility gap limits the formation of many useful single-phase alloys. In the case of nano-sized particles, the increased energetic contribution from the specific heterophase interfaces promotes miscibility as per the Gibbs-Thompson effect[11]. Researchers have also shown that the nanowire morphology also promotes solid solubility due to strain relaxation effects[12]. Strain relaxation is primarily due to the possibility of unconstrained lateral expansion/contraction in nanowires. Achievement of elemental

miscibility in nanowires is highly relevant as it potentially can synergize with morphology to produce usable devices.

As mentioned earlier, with respect to technological utility, one crucial challenge is the synthesis of nano-sized systems with an approprate synergy of morphology, size, and microstructure. A simple way to acquire such combination is by fixing two attributes (morphology and size) and manipulating the third one (microstructure) either by systematic variation of parameters during synthesis or by post-synthesis processing. For example, for the specific case of nanowire synthesis, size (aspect ratio) and morphology can be fixed using a template-assisted synthesis route where nanowires are bound to nucleate and grow inside the template pores, thus assuming the aspect ratio of the template pore. Therefore, The size (nanowire diameter) and morphology get fixed. Under an assumption that the overall composition of the nanowires remains the same, the microstructure (microstructural component's (phases) volume fraction, size, arrangements, design, composition, and size distribution, etc.) can be varied by treatments such as aging of initially deposited nanowires with a non-equilibrium microstructure. The growth kinetic can also be controlled during the synthesis process to isolate specific microstructures. One popular technique that utilizes a template for synthesizing nanowires is the electrodeposition technique[13]. The electrodeposition route has been extensively used to synthesize non-equilibrium structures. Researchers have shown that the electrodeposition process can be use to synthesisze amorphous-films, which, upon following annealing, can produce nano-crystalline microstructures. The controlled evolution of nanocrystalline microstructure can facilitate size-dependent formation and stabilization of specific phases. Furthermore, electrodeposition is a cost-effective and non-equipment intensive technique.

Therefore, this work Ag-Ni nanowires with varying compositions and microstructures were produced using a cost-effective template-based electrodeposition method. The main focus of the work is to address the miscibility of Ag and Ni atoms at the nanoscale and to investigate the role of electrodeposition process variables on microstructural evolution.

## 2. Materials and Method

### 2.1 Electrodeposition process

Fig. 1 illustrates the electrodeposition set-up used to synthesize the nanowires. An electrolyte solution, working and counter electrodes, and a power supply source are required in the Electrodeposition process. Details of the electrodeposition process are discussed in the ensuing paragraphs. The Ag-Ni nanowires were electrodeposited in an alumina template attached to the copper substrate, acting as a cathode.

#### 2.1.1 Electrolyte solution

In the present work, three types of electrolytic solutions were used to prepare Ag-Ni nanowires of different compositions. These solutions were prepared by dissolving salts in 100ml of distilled water. The different types of electrolytes used are given in the tables.

***Table 3-1****Electrolyte, composition of 50at% Ni*

| **Bath Composition** | **Concentration in g/100ml** | **Operating parameters** |
|---|---|---|
| $AgNO_3$ | 0.169 | Current, I = 3 and 1 mA,<br>Temp (°C) = Room temp.<br>pH = 3.6 |
| $NiNO_3.6H_2O$ | 0.25 | |
| $H_3BO_3$ | 0.03 | |
| Thio-Urea | 0.35 | |

***Table 3-2****Electrolyte, composition of 70at % of Ni*

| **Bath Composition** | **Concentration in g/100ml** | **Operating parameters** |
|---|---|---|

| | | |
|---|---|---|
| $AgNO_3$ | 0.169 | Current, I = 3mA,<br>Temp (°C) = Room temp,<br>pH = 3.6 |
| $NiNO_3.6H_2O$ | 0.68 | |
| $H_3BO_3$ | 0.03 | |
| Thio-Urea | 0.35 | |

All the salts of analytical grade were used. pH of the electrolytic solution was maintained at 3.66 by adding NaOH and $HNO_3$. Nanowires of compositions 50at % Ni, 70at % Ni and 85at % Ni were obtained from these three electrolytes, respectively. $AgNO_3$ and $NiNO_3$.6H2O were used to supply Ag and Ni ions. These salts are highly water soluble. Boric acid is used as a buffering agent, while TU facilitates the co-deposition of Ag and Ni. TU forms complexes with silver which results in a decrease in the reduction potential of silver.

### 2.1.2 Working and counter electrodes

A platinum foil (2cm x 2cm x 0.3cm) and a copper foil (4 cm x 3 cm x 0.3 cm) attached to the rear of the anodisc wer used as anode and cathode. The copper cathode was polished and ultrasonically cleaned and wiped using tissue paper before deposition.

### 2.1.3 Template

Commercial alumina membrane (Whatman) (pore size=200nm), a nominal thickness (60-65µm) was used as template to grow nanowires.

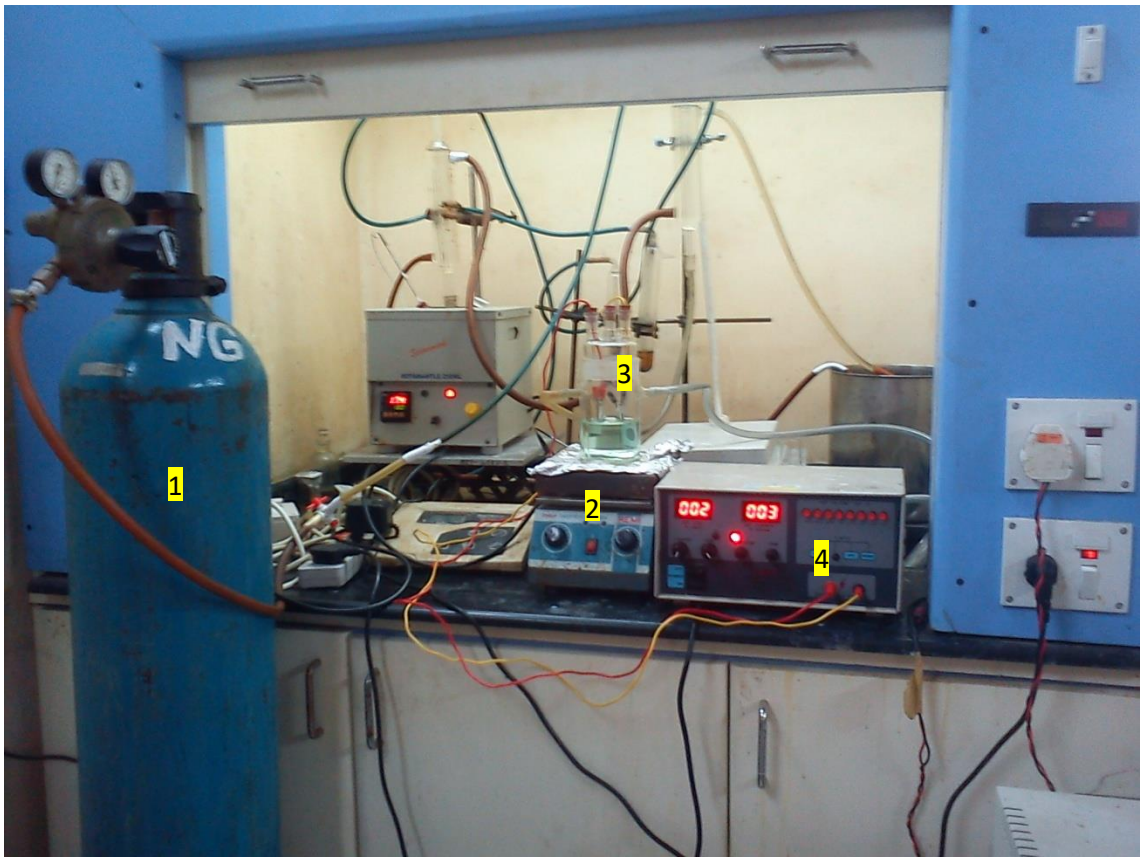


***Figure 1:*** *A schematic diagram of the electrodeposition unit.*

1. Argon gas cylinder

2. Magnetic stirrer

3. Electrolyte cell

4. Power source

## 2.2 Template Synthesis

To exploit the numerous interesting properties, various methods have been developed over the years to synthesize single and multi-component nanowires. Some of the popular synthesis methods are template-assisted synthesis[14], [15], the vapor-liquid-solid mechanism of anisotropic crystal growth[16], and the bottom-up synthesis approach[17]. Fundamentally, all the methods can be grouped under two categories-

1) Top-down approach
2) Bottom-up approach

As mentioned, both categories have characteristics that define nanowires' morphology and properties. The morphology and properties of nanowires depend on the choice of technique used for their fabrication. In the Top-down approach, nanowires are formed by removing materials from bulk, whereas the bottom-up approach involves the growth of seeds along specific crystallography directions [17]. In either case, quantity and quality should be balanced to achieve the preferred nanowires attributes. A top-down approach involving a series of pattern writing and etching steps gives excellent control over nanowires' shape and orientation and can be used several times. But the quality of nanowires suffers during this process because the etching steps involved cause surface roughness. On the contrary, this bottom-up technique produced high-quality nanowires through strain relaxation. Out of all bottom-up strategies, the template-based approach is one of the most simple, versatile, and intuitive ways to fabricate nanowires. It is commonly used to prepare free-standing nonoriented, and oriented nanowires, nanotubes, or nanorods. These templates contain tiny uniform cylindrical pores embedded in the host matrix. Desired materials are filled in the pores in various ways, which adopt the pore morphology to form nanowires. The most commonly used and commercially available templates include anodic alumina ($Al_2O_3$) [18], ion track-etched polymers[19], nanochannel glass[20], and mica films[21]. These templates have very high pore density (up to $10^9$ pores/$cm^2$) and minimal interpore distance. Templates having pore sizes ranging from 20-500 nm can be easily made. Template materials should be compatible with the processing environments. It should be chemically inert, thermally, and mechanically stable during the synthesis [22]. Porous alumina templates are produced by a two-step anodization process[23]. High-purity alumina foil is used as the starting material. Alumina foils are anodized

in various acids for a long duration, followed by subsequent dissolution, which leads to the formation of uniform hexagonal arrays of pores.

Template-based synthesis of nanowires has many advantages over other methods[24]

(1) This process does not require rigorous conditions, i.e., high temperature, high vacuum, and sophisticated instruments.
(2) It gives a high density of nanowires.
(3) This method gives the flexibility to form nanowires of different diameters.
(4) It allows the formation of multilayered nanowires.

However, there are certain disadvantages of this method, like AAO templates are not stable at a temperature above $50^0$C, careful handling of templates is required; otherwise, extremely brittle templates can break, and even a very small crack are undesirable that can cause failure of wire formation because deposition is centered in that region.

A schematic outlining the Template process for creating patterned nanowires is shown in Fig.2.

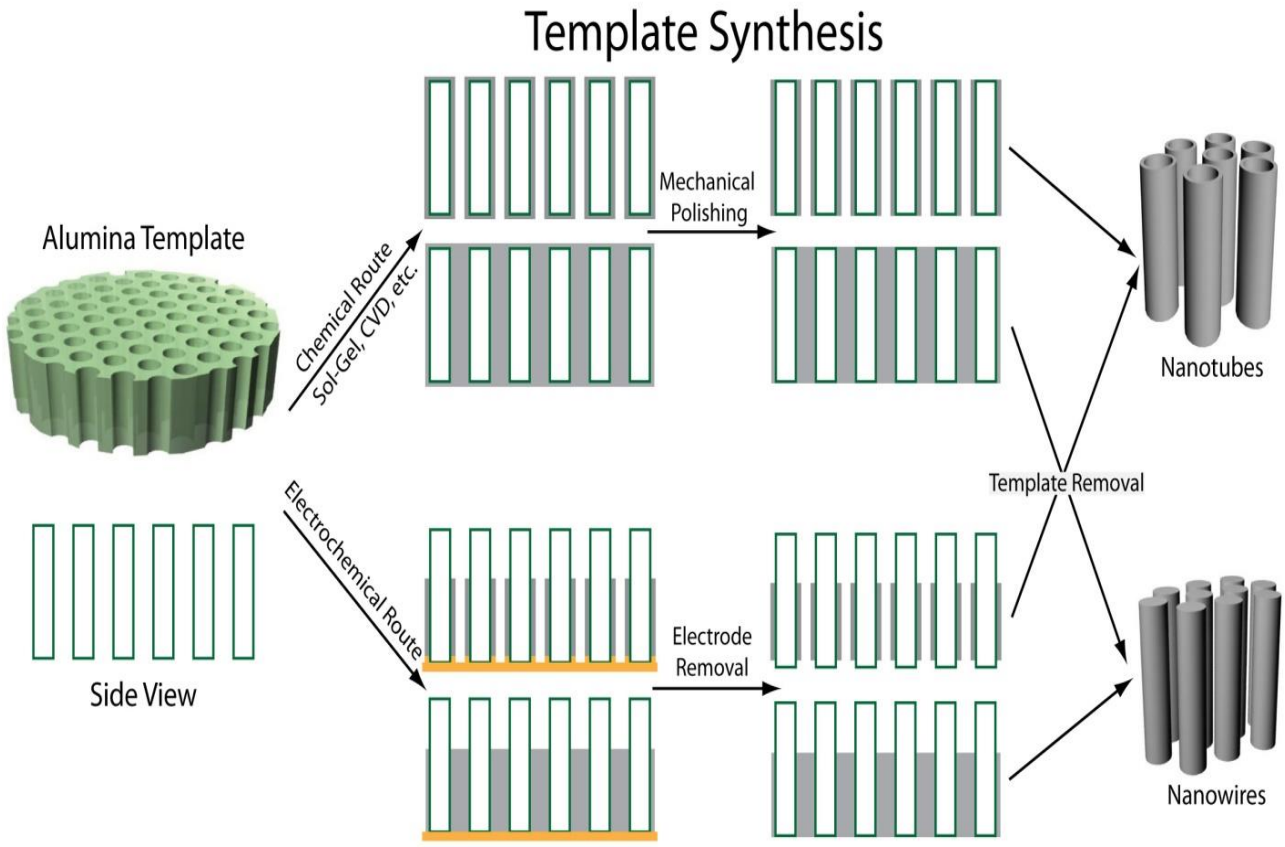


***Figure 2:*** *Schematic diagram of the template synthesis taken from reference* [25].

**Steps involved in Template-based synthesis of nanowires**:

Step 1 Anodic alumina template (anodic) or polycarbonate membrane is cleaned with acetone to remove dust particles.

Step 2 One side of the template is coated by a thick layer (approximately 200nm) of gold/silver, which serves as a cathode.

Step 3 Electrodeposition of chosen materials into the pores of the template by using electrodeposition set-up.

Step 4 Templates are dissolved to get free-standing nanowires for further characterization.

Thongmee et al. [26] have successfully synthesized metals (Ni, Co, Cu, and Fe) by electrodeposition. They have shown that how electrode potential alter the microstructure and magnetic behaviour. Leprince et al. [27] have prepared ZnO nanowires (130-150nm in diameter and 2-3um in length) by template (polycarbonate membranes)-based electrochemical deposition technique. They observed that ZnO nanowires were single crystals and had wurtzite structures. They have also reported that the quality of nanowires prepared via the template method critically depends upon the quality of pores. Kalska et al. [28] have synthesized iron nanowires by electrochemical method (using anodisc). They tested the materials' stability by putting them in different solutions, e.g., white wine, citric acid, 0.9% NaCl, distilled water, and ethanol, for 1-3 weeks. Funda et al. [25] have grown NiFe nanowires via template-based DC electrodeposition for different deposition times and pH values. They have reported that the length of NiFe nanowires increases with increasing deposition time. They have also said that the hysteresis loop changes with deposition time and pH; hence magnetic properties of wires can be improved by optimizing the deposition time and pH of the solution. Atalay et al. [29] have reported the electrodeposition of cobalt + nickel + iron nanowires in an aqueous sulfate solution via template-based synthesis. They have said that the back electrode placed on the AAO template plays the leading role in obtaining nanowires or nanorods. Sauer et al. [23] have synthesized highly ordered silver nanowires of diameter ranging between 30 to 70 nm by pulse electrodeposition in alumina templates. They reported that pulse electrodeposition was a very efficient method of synthesis of silver nanowires, and almost 100% of pores were occupied by silver. Sarkar et al. [30] have reviewed nanowires' physical and chemical properties and the most common synthesis approach of nanowires, i.e., template-based electrodeposition. Cheng et al. [31] successfully prepared pure Ni and Ni-Co using DC electrodeposition in conjunction with anodic alumina oxide (AAO). They have reported that the resistivity of alloy nanowires was increased with increasing Co content in Ni-Co nanowires.

## 2.3 Electrodeposition

The electrodeposition technique has gained considerable attention as a promising alternative nanowire preparation tool. This technique has been used for a long time to make thin films. It can

be extended to fabricate 1D nanostructure, as electrochemical growth can be easily controlled in the normal direction of the substrate. In the electrochemical synthesis of nanowires, one side of the template is coated with a thin conducting layer of metal, which serves as a cathode for electroplating.

Electrodeposition is a process in which an electric field moves metal ions in a solution to deposit on an electrode[13]. The method uses DC current to reduce cations of a desired material from a aquous or fused salt solution and alow them to deposit on a cathode as a thin layer. An electrolyte solution, working and counter electrodes, and a power supply source are required in the Electrodeposition process. Electrolytes contain various metallic salts and other ions that fascilitate the electricity flow. A power supply system supplies a DC current which causes dissolved metal ions to deposited at the cathode.

The Nernst equation describes the electrode potential:

$$E = E_0 + \frac{RT}{nF} \ln(a_i) \quad (1)$$

Where $E_0$ is the standard electrode potential, F and, R are Farady and gas constant respectively. T denotes temperature.

When deposition is confined inside the pores of templates, nanowires are produced. On removal of templates, free nanowires are obtained. The template used in the electrochemical deposition process should be compatible and stable in the electrolyte. Track-etched mica films, or AAO, are commonly used as a template for electrodeposition. This method has been used to synthesize a wide variety of nanowires.

This process has a significant advantage over others in fabricating a multilayer structure.

## 2.4 Ag-Ni Electrodeposition

This section provides a brief review of Ag-Ni electrodeposition.

Liang et al. [33] have reported the electrodeposition of Ag-Ni thin films on the copper substrate from a thio-urea-based acidic solution. They have reported that the thiourea strongly tends to form complex with silver and bring down its reduction potential closer to nickel. They have also reported that thiourea complexes dissociated during nickel electrodeposition, which leads to sulfur incorporation into the films. The deposition films were fine-grained and had multiple phases. They reported that these phases were metastable and separated into two different elemental phases annealed at 600C.

Santhi et al. [34] successfully prepared nanocrystalline Ag-Ni thin films on stainless steel substrate using the pulse electrodeposition technique. They have reported that Ag-Ni films are metastable, and the amount of nickel in the film was increased with increasing current density. They have also studied the magnetic properties of films and observed that Ag-Ni films were ferromagnetic even at room temperature. In the same study, they reported that the co-deposition of Ag and Ni is facilitated by adding TU, which forms a complex with silver and reduces its reduction potential.

Bdikin et al. [35] have electrodeposited $Ag_xNi_{1-x}$ (x=0 -1) thin films on a copper substrate using a single electrolyte containing Ag and Ni ions. The researchers showed that films were nanocrystalline mixtures of pure silver and nickel. They have also reported that films were metastable and dissociated into a single elemental phase upon annealing at 600C.

Eom et al. [36] have synthesized Ag-Ni thin film on the brass substrate. They showed the effect of current density and electrolytic concentration on the crystallography of Ag-Ni thin films. They have observed that Ni content increases with increasing current density due to the mass transfer limitation of Ag ions. While morphology also changed from dendrite to particle type when current density increased from low to high.

From these studies, it is found that the process variables for Ag-Ni electrodeposition are current density, pH, temperature, and additive, which play a crucial role in determining the film compositions, grain size, morphology, and phase fraction of different phases. Some of these parameters are briefly described below:

### 2.4.1 Effect of current on the solubility

Electro-crystallization theory relates over potential with a current density as follows

$$\eta = a + b \log i \quad (2)$$

Equation (2) is the popular Tafel equation[37]. Where$\eta$ is over potential, a and b are constants, and i is the current density.

According to equation (2), over potential increases with current density, at high over potential current density would be high, which enhances the nucleation process and results in fine grain deposits[36]. The nucleation rate J is given by eqn. 3

$$J = K_1 . \exp\left[\frac{-bs\varepsilon^2}{zekT\eta}\right] \quad (3)$$

Where $K_1$ is the rate constant, b is the geometrical factor, s is the area occupied by one atom on the surface of the cluster, $\in$ the specific edge energy, z is the electronic charge of the ion, e is the electronic charge, k is the Boltzmann constant, and $\eta$ the overpotential.

From equation(3) and equation (2), it is clear that the nucleation rate increases with current density, which leads to a finer particle size that promotes the extent of solid solubility according to the Gibbs-Thompson effect.

### 2.4.2 Effect of additives (TU)

Since Ag and Ni have a big difference in their standard potentials, co-deposition of Ag-Ni is very difficult. Silver is preferentially deposited at the onset of nickel deposition. Schmidt et al. [38] have shown that the thiourea (TU) has the strongest complexing capacity with silver. It has a tendency to form coordinate bonds with many univalent and multivalent ions. When TU is added

to the electrolyte during the electrodeposition of Ag-Ni, it forms complexes with silver and decreases the reduction potential of silver to a negative value without altering the nickel deposition process. It also improves the morphology of the silver matrix and favors the nickel incorporation into the deposit.

## 3. Results and Discussion

### 3.1 Ag-Ni nanowires with average composition of 50at %Ag deposited for 30 minutes.

Ag-Ni nanowires were electrodeposited using constant current input of 3mA for 30 minutes. SEM & low magnification TEM micrographs of the electrodeposited mass shown in figure 3(a) and 3(b). The diameter of the wires is approximately 200 nm. The average composition of the deposited mass was ~50 at% Ag.

TEM-based analysis was used to characterize further the crystal structure, microstructure, and composition of individual nanowires. Qualitative information about the phase and/or compositional heterogeneity was also ascertained from Z-contrast images using a HAADF- STEM mode [46]. Compositional inhomogenity, if present, will exhibits a composition-dependent image contrast. The STEM-HAADF image of nanowires of interest is dipicted in Figure 4. Fig. 4 reveals domains having varrying contrast in the microstructure, ascertaining the compositional heterogeneity.

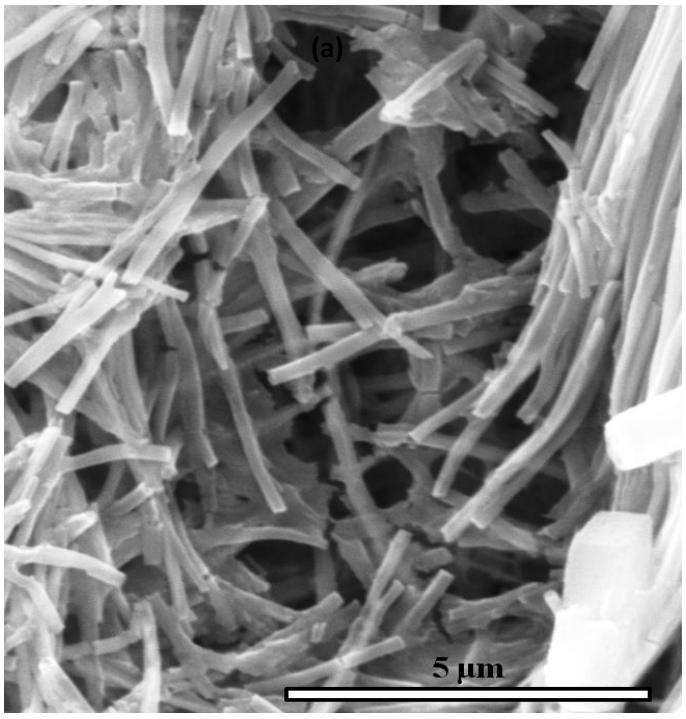
(a)
5 µm

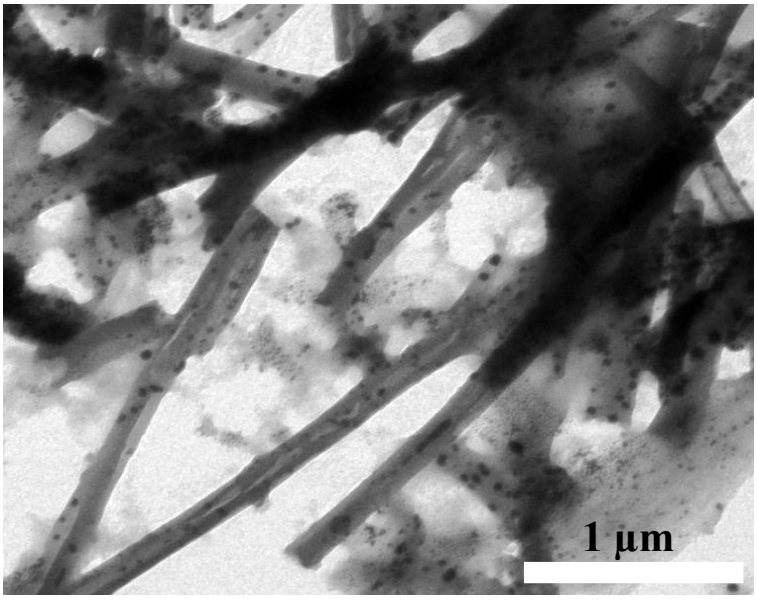
1 µm

(b)

***Figure 3:*** *(a) SEM image and, (b) TEM bright field image of as deposited nanowires.*

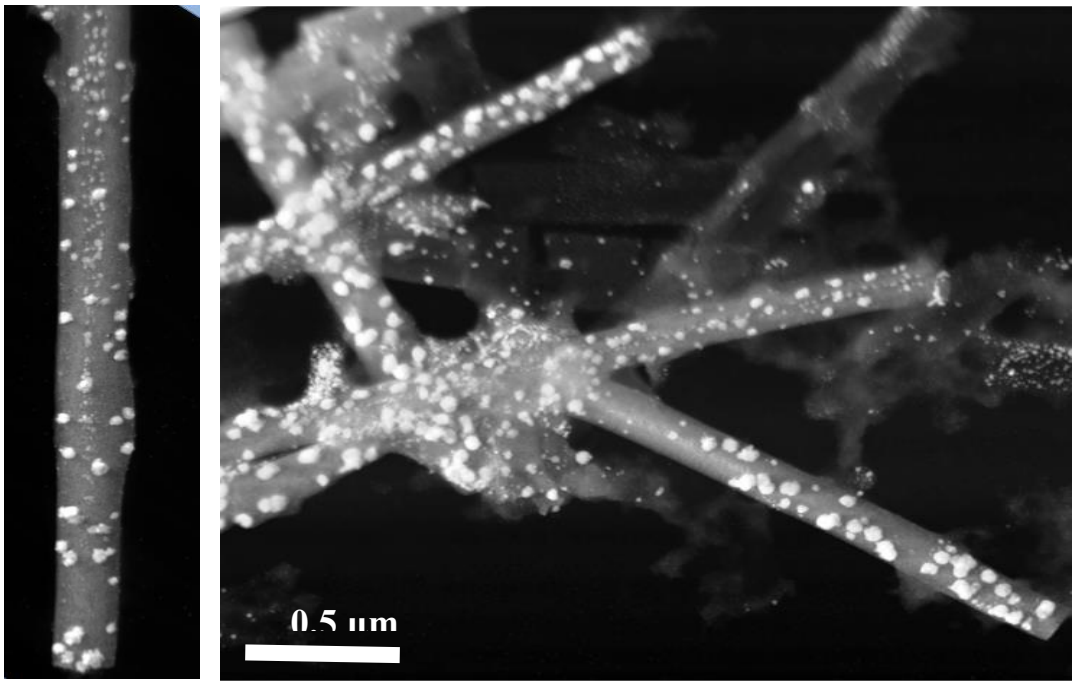


***Figure 4:*** *STEM-HAADF image.*

STEM-HAADF images (Fig. 4) shows that the microstructure of the as-deposited nanowire consists of spherical nanoparticles distributed in a matrix. Compositional line profile analysis (Fig. 5) was conducted to investigate the compositional identity of the microstructural components. Figure 5 (a) shows the STEM-HAADF micrograph (the nanowire). Figure 5(b) and 5(c) plots $Ag_L$and$Ni_K$ characteristic X-ray counts obtained from different points along the line AC and KM.

The line profile in Figure 5(b) shows that the matrix contains fairly uniformly distributed Ni and Ag atoms. The profiles in the Figure 5(c) indicate that the nanoparticles are basically Ag-rich.

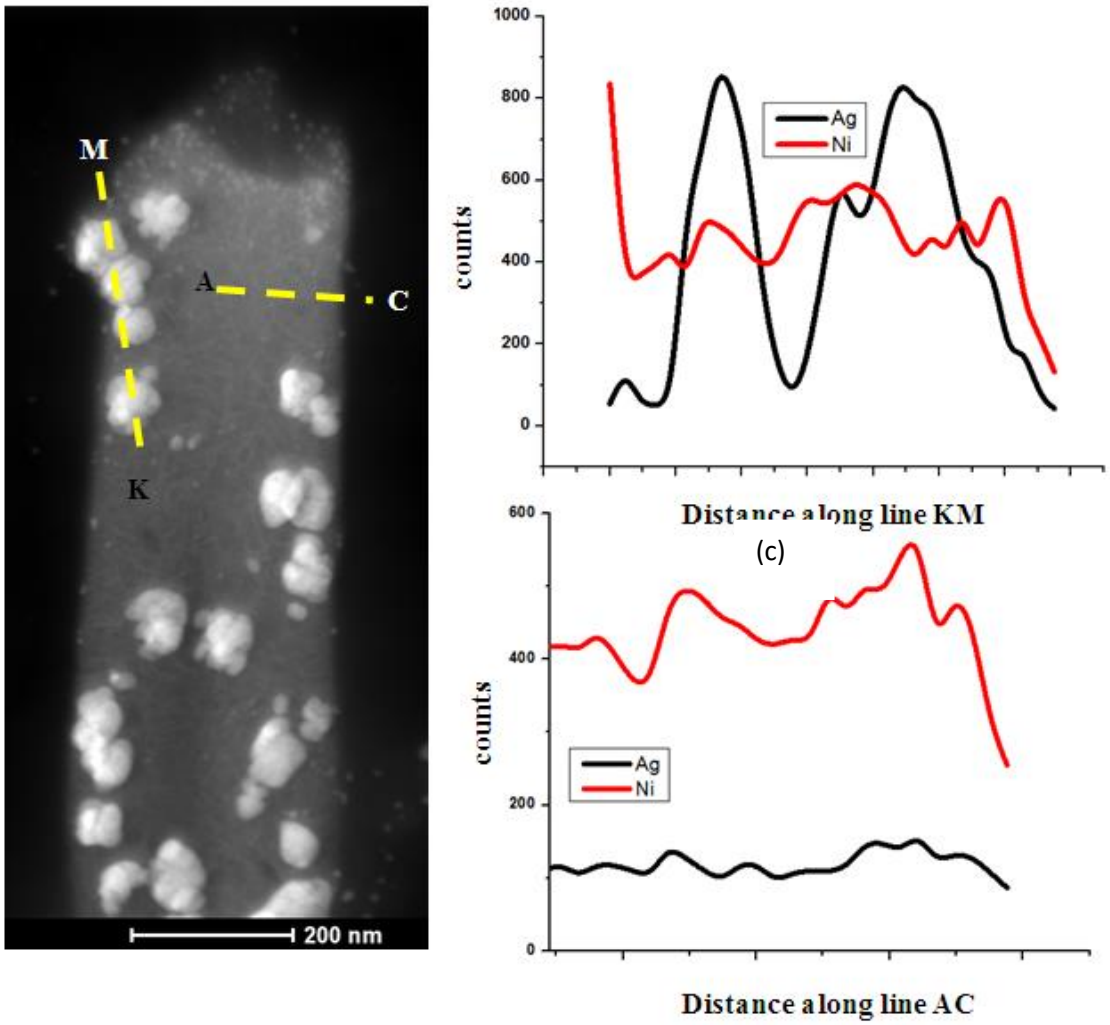


(a) (b)

***Figure 5:*** *(a) STEM image (b) A plot of counts of Ag and Ni characteristic X-ray signals along the line AC denoted in the STEM image (c) A plot of counts of Ag and Ni along the line KM.*

High resolution TEM bright field image HRTEM of a representative region inside a nanowire is shown in figure 6. The HRTEM micrograph shows image of two nanoparticles and the embedding matrix. The presence of continuous lattice fringes along particles indicated that the particles are crystalline in nature. However, these fringes are missing in the matrix phase which

indicates that it is amorphous. The d-spacing calculated from the FFT is 2.28Å. The value of d-spacing is not matching with the actual d-spacing of pure Ag phase (for the (111) plan). The observation indicated that the crystalline particles in the matrix contains Ag-rich, Ag-Ni solid solution phase. Combining results obtained from compositional line analysis and HRTEM analysis, it can be concluded that the as synthesized nanowire has two phase microstructure.Matrix of nanowire is made-up with both silver and nickel and is amorphous in nature whereas embedded particles are crystalline in nature containing Ag-Ni solid solution phase.

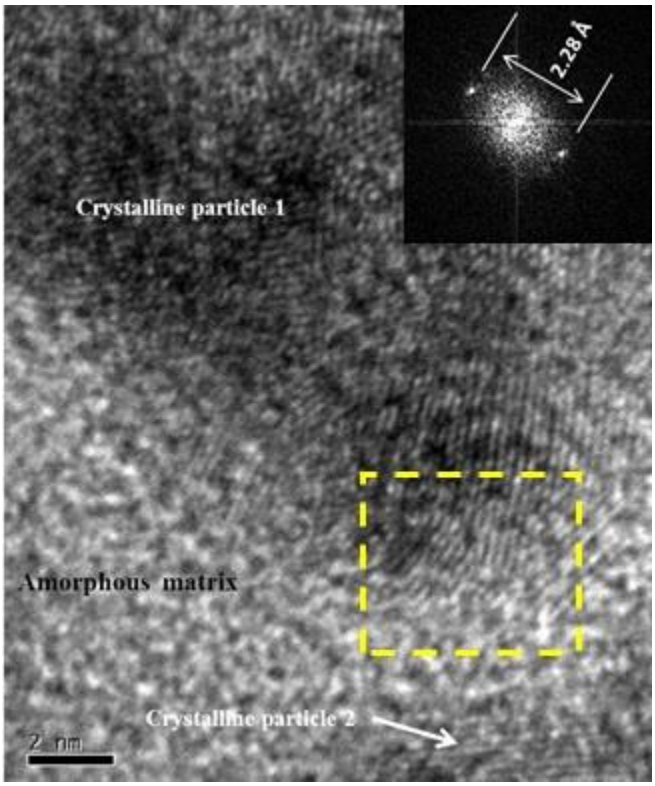


***Figure 6:*** *HRTEM image of particle and the matrix phase.*

## 3.2 Ag-Ni nanowires with an average composition of 50at %Ag deposited for 1 hour and 45 minutes.

Ag-Ni nanowires were electrodeposited using constant current input of 1mA for 1 hour and 45 minutes. SEM & low magnification TEM micrograph of the electrodeposited mass is shown in Figures 7 (a) and 7 (b). It can be shown from Figures 7(a) and 7(b) that experiment has produced a high yield of nanowires. The SEM-EDS-based compositional analysis shows that the average composition of as-deposited nanowires was 50at % Ag and 50at % Ni. A high-magnification TEM bright field image of the representative nanowire is shown in Figure 8(a). It can be shown from Figure 8(a) that the microstructure of the nanowire is composed of nearly spherical particles embedded in a matrix. The high-resolution TEM bright field (HRTEM) image of the representative area is shown in Figure 8(b). The HRTEM image shows lattice fringes in the region of nanoparticles, whereas no such fringes along the matrix of the nanowire. The HRTEM image clearly indicates that the matrix of nanowires is an amorphous phase, while embedded nanoparticles are crystalline in nature. The study of the TEM bright field image and HRTEM image indicates that the microstructure of as-deposited nanowires is almost similar to the previous result; the only difference, in this case, is the size of the nanoparticles embedded in the matrix.

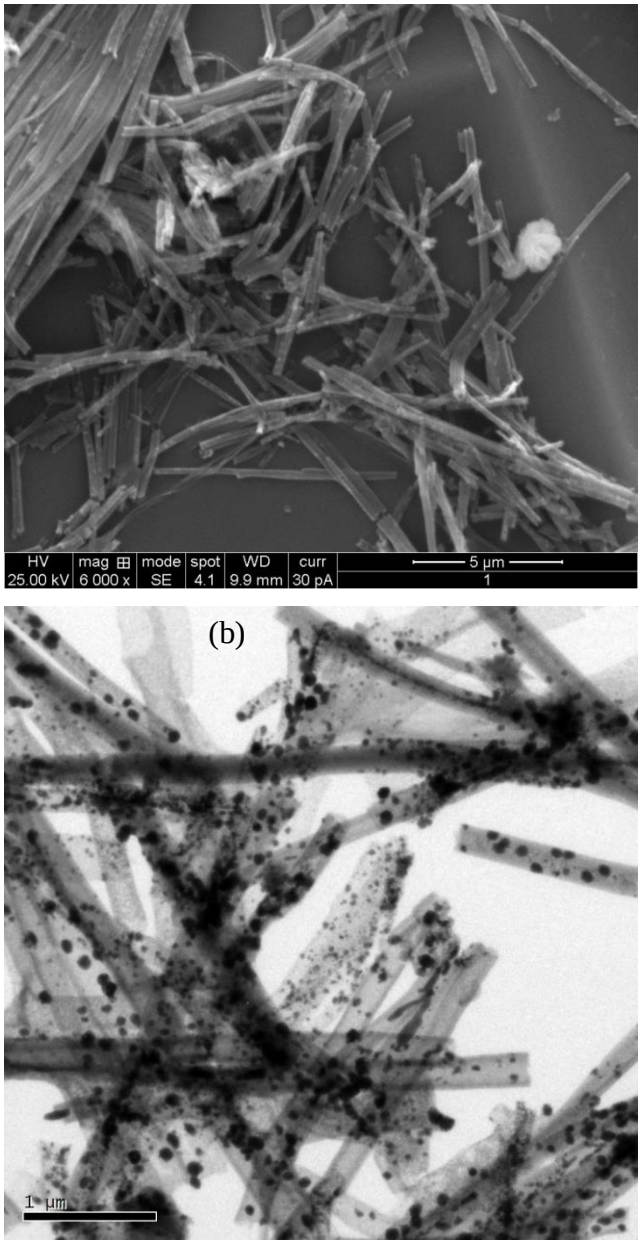


***Figure 7:*** *(a) SEM micrograph and, (b) TEM micrograph of deposited nanowires.*

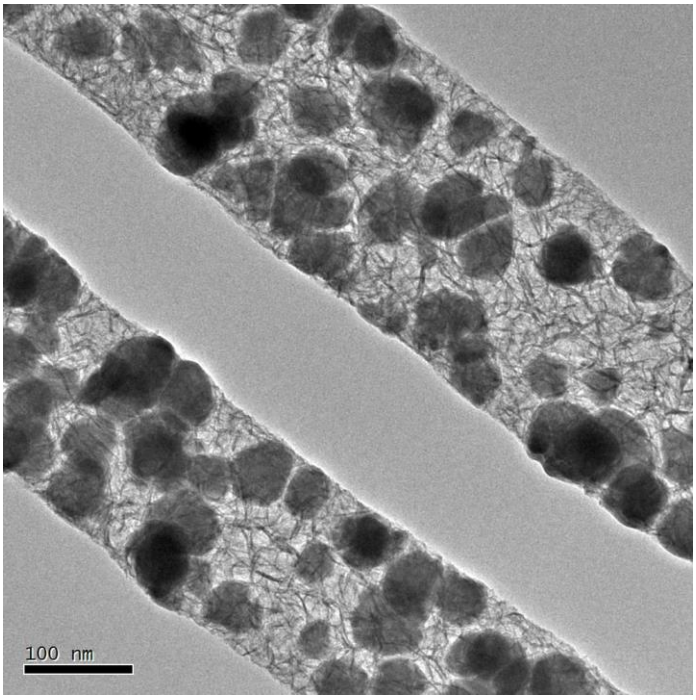


(a)

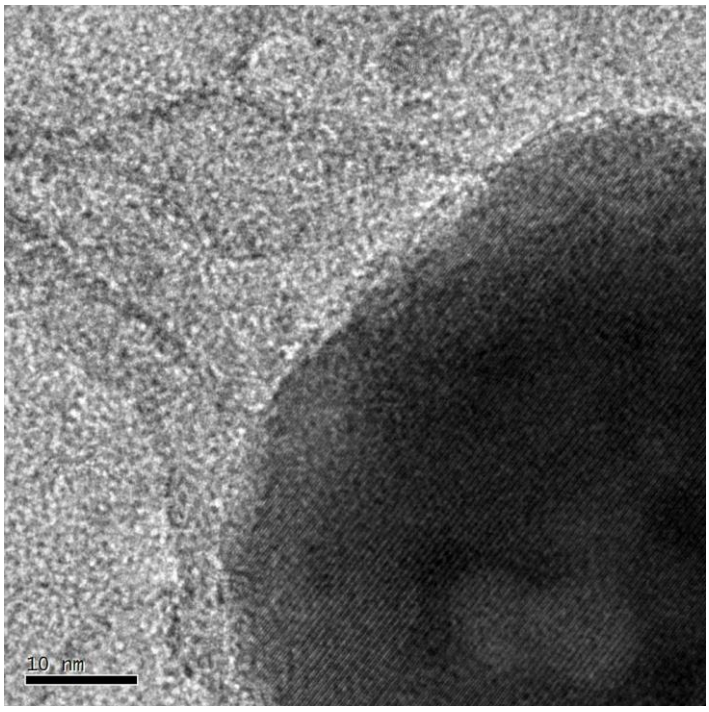


(b)

***Figure 8:*** *(a) TEM bright field and (b) HRTEM image of the nanowire.*

### 3.3 Microstructure of Ag-Ni nanowires of composition 30at % Ag and 70at % Ni, electrodeposited for 30minutes.

Ag-Ni nanowires were electrodeposited at constant current input of 3mA for 30 minutes at RT and under inert atmosphere. SEM & low magnification TEM micrograph of the electrodeposited mass shown in Figures 9 (a) and 9 (b). The SEM-EDS-based compositional analysis of deposited nanowires shows the average composition of nanowires as 70at % Ni. Distinct diffraction contrasts were observed across the nanowire diameter (Fig. 9b), confirms a two-phase microstructure. A representative STEM-HAADF image ( Figure 10) also indicating the presence of compositional heterogeneity.

(a)

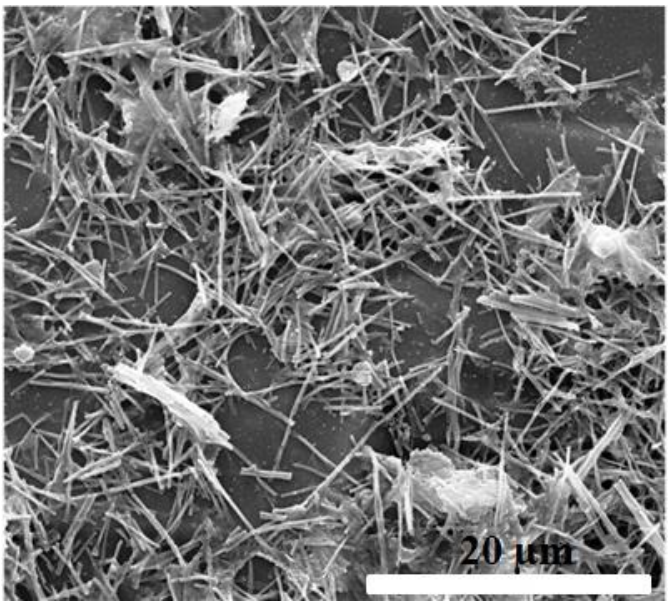

(b)

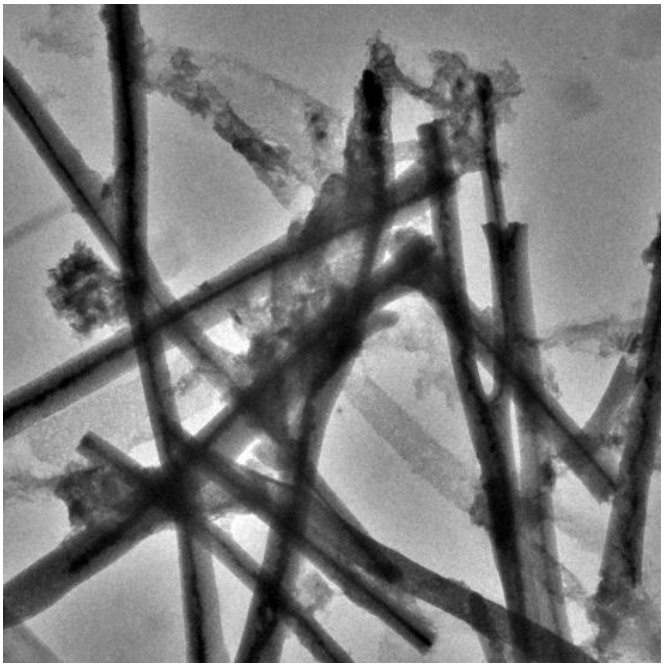

***Figure 9:*** *(a) SEM micrograph and, (b) TEM image of nanowires.*

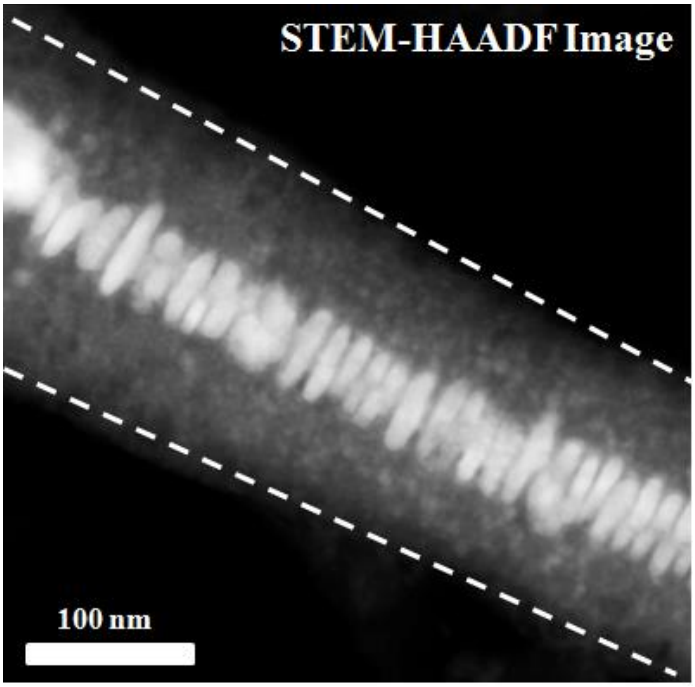

***Figure 10:*** *A STEM-HAADF image of the representative nanowire.*

The result from compositional mapping is shown in Figure 11. Figures 11(a), 11(b), and 11(c) provide STEM-HAADF images, Ni compositional maps, and Ag compositional maps, respectively. It can be seen from the compositional mapping images that the Ni atoms are fairly distributed throughout the nanowire; however, Ag is primarily present in the central region. A bright contrast along the axis of the nanowire is due to the presence of higher Ag content in that region. Line compositional analysis was conducted along the diameter of nanowires shown in Figure 11(d). Results from the compositional line profile were provided in Figure 11(d), which provides the counts of the Ag-characteristic X-ray signal along the nanowire diameter. Line profile analysis confirms that Ag is primarily present in the central region.

(a)

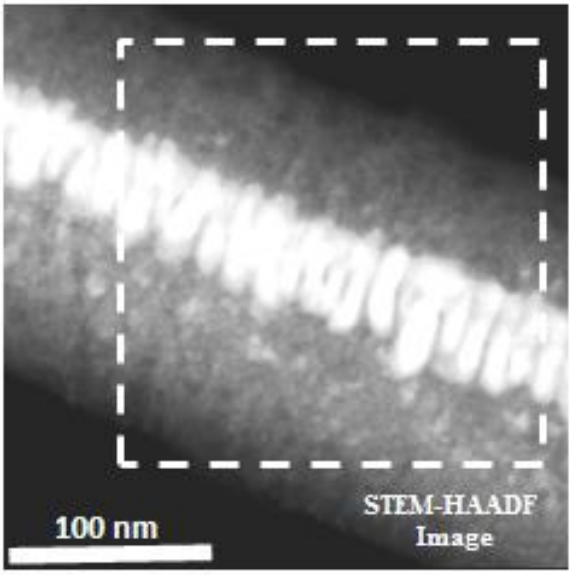


(b)

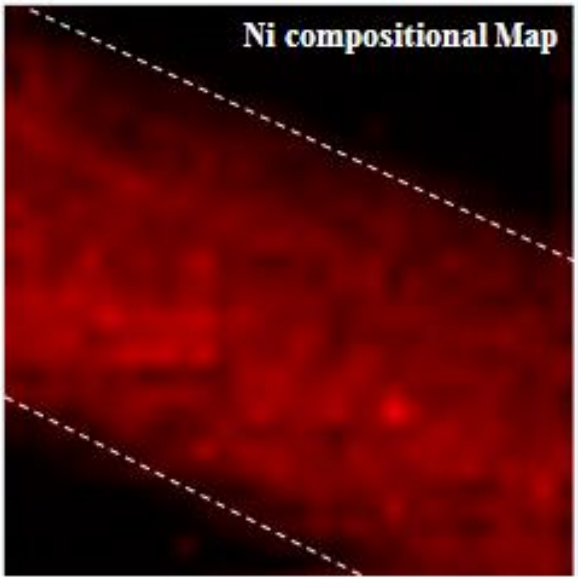


(c)

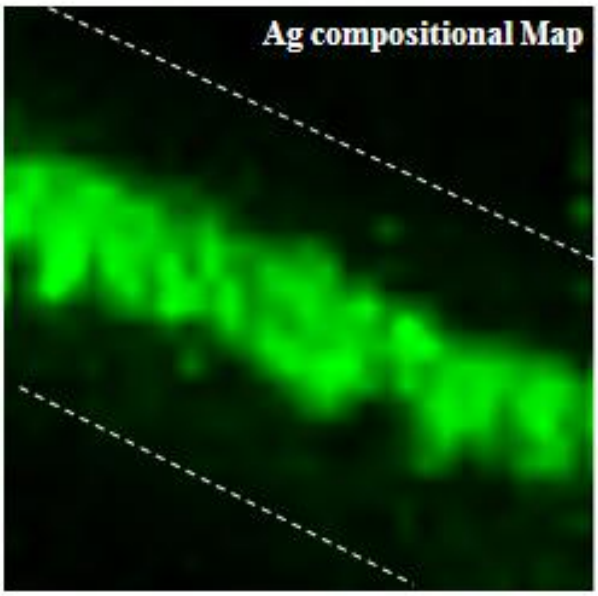


(d)

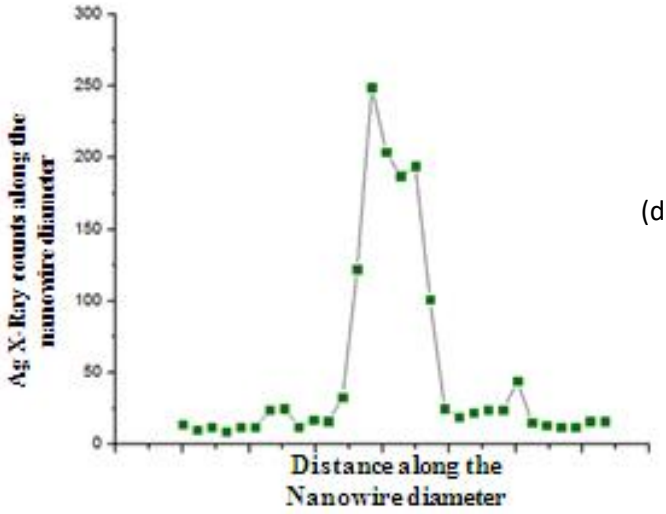


***Figure 11:*** *(a) STEM image, (b) Ni compositional image, and (c) Ag compositional image (d) A plot of counts of Ag-characteristic X-ray signals along the diameter of nanowire.*

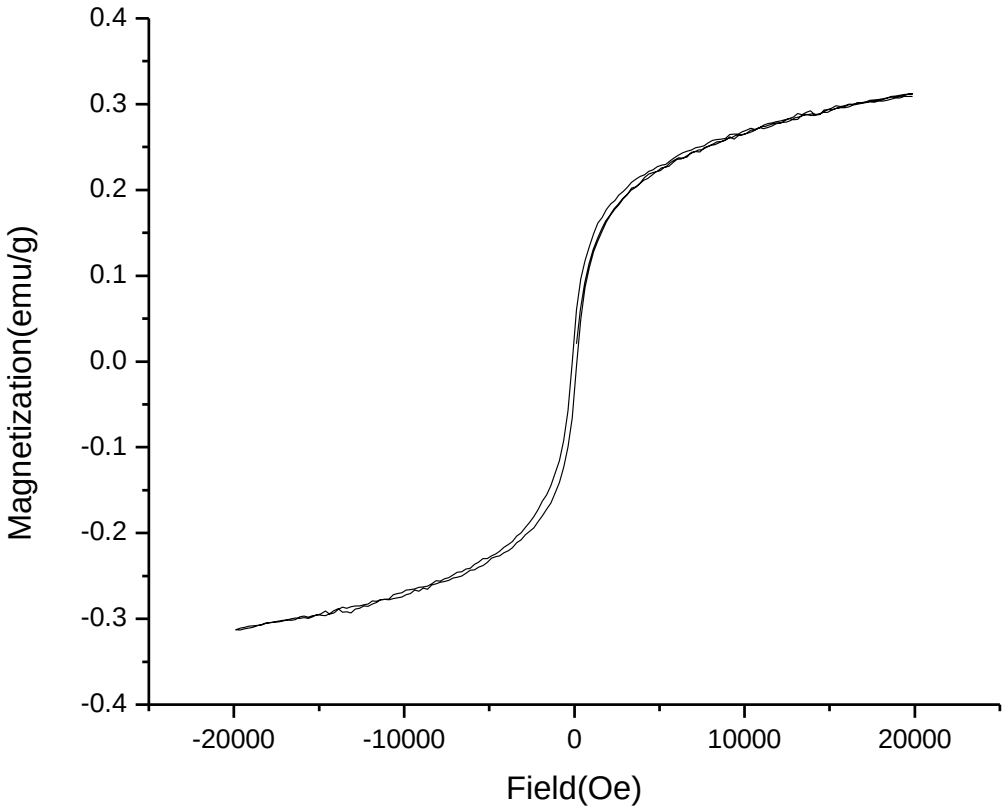


***Figure 12:*** *Magnetization curve .*

The magnetization curve of as-deposited nanowires is shown in Figure 12. The absence of a diamagnetic component in the hysteresis loop clearly indicates the lack of a pure Ag phase. The compositional mapping and line profile results showed that the deposited nanowires adopted core-shell microstructure. The central region contains Ag-rich, Ag-Ni solid solution, whereas the peripheral region is Ni-rich, Ag-Ni solid solution.

## 3.4 Microstructure of Ag-Ni nanowires of composition 30at % Ag and 70at % Ni, electrodeposited for 1 hour 45 minutes.

Figures 13 (a) and (b) show the SEM and TEM images of deposited nanowires. The SEM and TEM images reveal nanowires with 200nm diameter. The SEM-EDS-based compositional

analysis of deposited nanowires shows the average composition of nanowires was 70at % Ni. TEM micrograph revealed distinct diffraction contrasts across the nanowire diameter, which indicate a two-phase microstructure. TEM image provided in Figure 14 shows that the nanowire has a core-shell microstructure with a very thick central region, which is greater than for nanowires grown for 30 minutes.

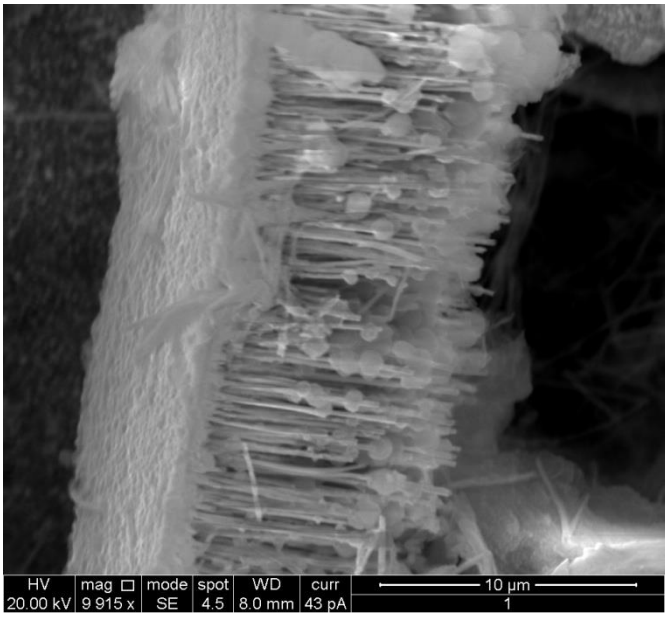


(a)

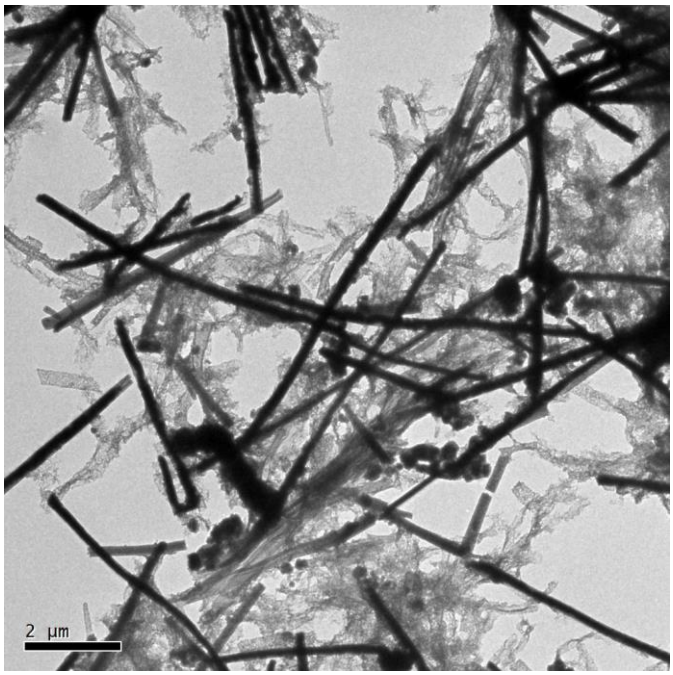


(b)

***Figure 13:*** *(a) SEM micrograph and, (b) TEM image of nanowires.*

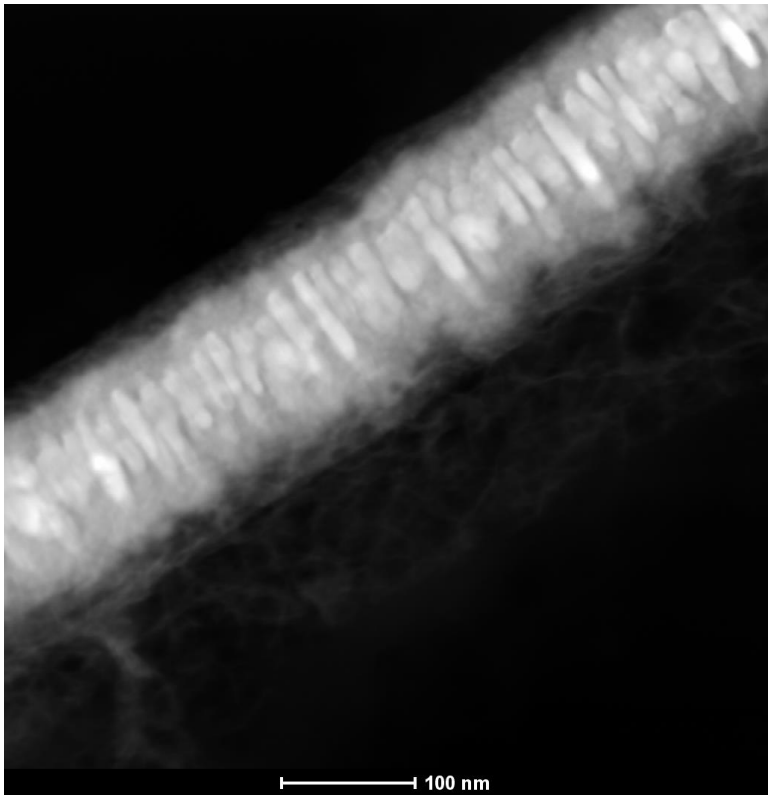


***Figure 14:*** *high magnification TEM image of a nanowire.*

# 4 Conclusions

The following conclusions are drawn from observation and analysis of results:

1. Ag-Ni nanowires with average composition 50at % Ag and 50at % Ni electrodeposited for 30minutes:
   Following key observations were made

   - The microstructure of as-deposited nanowires contained nearly spherical nanoparticles embedded in a matrix.

- Compositional and structural analysis shows that the matrix made up of Ag-Ni was amorphous in nature, while the embedded nanoparticles were Ag-rich crystalline phase.

2. Ag-Ni nanowires with average composition of 50at % Ag and 50at % Ni electrodeposited for 1hour45minutes:
    - It is observed that the as-deposited Ag-Ni nanowires have a two-phase microstructure. The microstructures of nanowires have relatively larger Ag-Ni nanoparticles embedded in an amorphous matrix.

3. Ag-Ni nanowires with average composition 70at % Ni electrodeposited for 30minutes:
    - As synthesized nanowires adopted a core-shell microstructure.
    - The microstructure of deposited nanowires contains two solid solution phases.
    - The central phase, which lies along the nanowires axis, contains a crystalline, Ag-rich solid solution Ag-Ni phase. The peripheral region was polycrystalline, containing nano-sized grains of predominantly Ni-rich, Ni-Ag solid solution phase.
4. Ag-Ni nanowires with an average composition of 70% Ni electrodeposited for 1hour 45minutes:
    - The Ag-Ni nanowires were prepared by electrodeposition technique. The nanowires have a core-shell microstructure with a very thick Ag-rich central region, more significant than the nanowires grown for 30 minutes.

## References


[1] Y. Nakayama, P. J. Pauzauskie, A. Radenovic, R. M. Onorato, R. J. Saykally, J. Liphardt, and P. Yang, "Tunable nanowire nonlinear optical probe," *Nature*, vol. 447, no. 7148, pp. 1098–1101, Jun. 2007.

[2] L. C. L. Y. Voon, Y. Zhang, B. Lassen, M. Willatzen, Q. Xiong, and P. C. Eklund, "Electronic Properties of Semiconductor Nanowires," *J. Nanosci. Nanotechnol.*, vol. 8, no. 1, pp. 1–26, 2008.

[3] X. Zhao, C. M. Wei, L. Yang, and M. Y. Chou, "Quantum Confinement and Electronic Properties of Silicon Nanowires," *Phys. Rev. Lett.*, vol. 92, no. 23, p. 236805, Jun. 2004.

[4] J. Pohl, C. Stahl, and K. Albe, "Size-dependent phase diagrams of metallic alloys: A Monte Carlo simulation study on order–disorder transitions in Pt–Rh nanoparticles," *Beilstein J. Nanotechnol.*, vol. 3, pp. 1–11, Jan. 2012.

[5] D. Josell, S. H. Brongersma, and Z. Tőkei, "Size-Dependent Resistivity in Nanoscale Interconnects," *Annu. Rev. Mater. Res.*, vol. 39, no. 1, pp. 231–254, 2009.

[6] W. A. Jesser and C. T. Schamp, "Nanoparticle semiconductor compositions in the miscibility gap," *Phys. Status Solidi C*, vol. 5, no. 2, pp. 539–544, 2008.

[7] J. Luo, L. Wang, D. Mott, P. N. Njoki, Y. Lin, T. He, Z. Xu, B. N. Wanjana, I.-I. S. Lim, and C.-J. Zhong, "Core/Shell Nanoparticles as Electrocatalysts for Fuel Cell Reactions," *Adv. Mater.*, vol. 20, no. 22, pp. 4342–4347, 2008.

[8] C. Srivastava, S. Chithra, K. D. Malviya, S. K. Sinha, and K. Chattopadhyay, "Size dependent microstructure for Ag–Ni nanoparticles," *Acta Mater.*, vol. 59, no. 16, pp. 6501–6509, Sep. 2011.

[9] S. Elzey and V. H. Grassian, "Agglomeration, isolation and dissolution of commercially manufactured silver nanoparticles in aqueous environments," *J. Nanoparticle Res.*, vol. 12, no. 5, pp. 1945–1958, Jun. 2010.

[10] R. E. Reed-Hill, *Physical metallurgy principles*, vol. 29. Van Nostrand New York, 1972.

[11] D. A. Porter and K. E. Easterling, "Phase transformation in materials," *Chapman Hall Bound. Row Lond.*, pp. 291–308, 1992.

[12] T. Kuykendall, P. Ulrich, S. Aloni, and P. Yang, "Complete composition tunability of InGaN nanowires using a combinatorial approach," *Nat. Mater.*, vol. 6, no. 12, pp. 951–956, Dec. 2007.

[13] J. B. Mohler, *Electroplating and related processes*. Chemical Pub Co, 1969.

[14] D. Routkevitch, T. L. Haslett, L. Ryan, T. Bigioni, C. Douketis, and M. Moskovits, "Synthesis and resonance Raman spectroscopy of CdS nano-wire arrays," *Chem. Phys.*, vol. 210, no. 1–2, pp. 343–352, Oct. 1996.

[15] C. A. Huber, T. E. Huber, M. Sadoqi, J. A. Lubin, S. Manalis, and C. B. Prater, "Nanowire Array Composites," *Science*, vol. 263, no. 5148, pp. 800–802, Feb. 1994.

[16] R. S. Wagner and W. C. Ellis, “VAPOR-LIQUID-SOLID MECHANISM OF SINGLE CRYSTAL GROWTH,” *Appl. Phys. Lett.*, vol. 4, no. 5, p. 89, 1964.

[17] B. Gates, Y. Yin, and Y. Xia, “Magnetochromatic microspheres: rotating photonic crystals,” *J Am Chem Soc*, vol. 122, pp. 12582–12583, 2000.

[18] S. H. Park and Y. Xia, “Fabrication of Three-Dimensional Macroporous Membranes with Assemblies of Microspheres as Templates,” *Chem. Mater.*, vol. 10, no. 7, pp. 1745–1747, Jul. 1998.

[19] R. R. L. Fleischer, P. B. Price, and R. M. Walker, *Nuclear Tracks in Solids: Principles and Applications*. University of California Press, 1975.

[20] A. Rosenberg, R. J. Tonucci, H.-B. Lin, and A. J. Campillo, “Near-infrared two-dimensional photonic band-gap materials,” *Opt. Lett.*, vol. 21, no. 11, pp. 830–832, Jun. 1996.

[21] C. R. Martin, M. Nishizawa, K. Jirage, M. Kang, and S. B. Lee, “Controlling Ion-Transport Selectivity in Gold Nanotubule Membranes,” *Adv. Mater.*, vol. 13, no. 18, pp. 1351–1362, 2001.

[22] G. Cao and D. Liu, “Template-based synthesis of nanorod, nanowire, and nanotube arrays,” *Adv. Colloid Interface Sci.*, vol. 136, no. 1–2, pp. 45–64, Jan. 2008.

[23] G. Sauer, G. Brehm, S. Schneider, K. Nielsch, R. B. Wehrspohn, J. Choi, H. Hofmeister, and U. Gosele, “Highly ordered monocrystalline silver nanowire arrays,” *J. Appl. Phys.*, vol. 91, no. 5, pp. 3243–3247, 2002.

[24] H. Singh, “Fabrication and Characterization of Copper Nanowires,” in *Nanowires - Implementations and Applications*, A. Hashim, Ed. InTech, 2011.

[25] F. E. Atalay, H. Kaya, S. Atalay, and S. Tari, “Influences of deposition time and pH on magnetic NiFe nanowires fabrication,” *J. Alloys Compd.*, vol. 469, no. 1–2, pp. 458–463, Feb. 2009.

[26] S. Thongmee, H. L. Pang, J. Ding, and J. Y. Lin, “Fabrication and magnetic properties of metallic nanowires via AAO templates,” *J. Magn. Magn. Mater.*, vol. 321, no. 18, pp. 2712–2716, Sep. 2009.

[27] Srivastava C, Rai RK. Two phase microstructure for Ag–Ni nanowires. Chemical Physics Letters. 2013 Mar 13;561:101-6.

[28] B. Kalska-Szostko, U. Wykowska, K. Piekut, and E. Zambrzycka, “Stability of iron (Fe) nanowires,” *Colloids Surfaces Physicochem. Eng. Asp.*, vol. 416, pp. 66–72, Jan. 2013.

[29] F. E. Atalay, H. Kaya, V. Yagmur, S. Tari, S. Atalay, and D. Avsar, "The effect of back electrode on the formation of electrodeposited CoNiFe magnetic nanotubes and nanowires," *Appl. Surf. Sci.*, vol. 256, no. 8, pp. 2414–2418, Feb. 2010.

[30] RK. Rai, MP Singh, C. Srivastava ,Synthesis and characterization of Ag–Co–Ni nanowires. Journal of Microscopy. 2014 Sep;255(3):169-73..

[31] S. L. Cheng, Z. H. Kuo, and C. H. Chung, "Structural and electrical properties of Ni and Ni-Co nanowires synthesized by electrodeposition in anodic alumina templates," in *Nanoelectronics Conference (INEC), 2011 IEEE 4th International*, 2011, pp. 1–2.

[32] D. Samal and P. S. A. Kumar, "Giant magnetoresistance," *Reson*, vol. 13, no. 4, pp. 343–354, Apr. 2008.

[33] D. Liang, Z. Liu, R. D. Hilty, and G. Zangari, "Electrodeposition of Ag–Ni films from thiourea complexing solutions," *Electrochimica Acta*, vol. 82, pp. 82–89, Nov. 2012.

[34] K. Santhi, S. N. Karthick, H.-J. Kim, M. Nidhin, V. Narayanan, and A. Stephen, "Microstructure analysis of the ferromagnetic Ag–Ni system synthesized by pulsed electrodeposition," *Appl. Surf. Sci.*, vol. 258, no. 7, pp. 3126–3132, Jan. 2012.

[35] I. K. Bdikin, G. K. Strukova, G. v. Strukov, V. v. Kedrov, D. v. Matveev, S. A. Zver'kov, and A. L. Kholkin, "Growth, crystal structure and stability of Ag-Ni/Cu films," *Mrs Online Proc. Libr.*, vol. 854, p. null–null, 2004.

[36] EOM Hyeonjin, JEON Byungjun, KIM Donguk, and YOO Bongyoung, *Electrodeposition of Silver-Nickel Thin Films with a Galvanostatic Method*, vol. 51. Sendai, JAPON: Japan Institute of Metals, 2010.

[37] M. Paunovic and M. Schlesinger, *Fundamentals of Electrochemical Deposition*. Electrochemical Society Series, 1998.

[38] W. U. Schmidt, R. C. Alkire, and A. A. Gewirth, "Mechanic Study of Copper Deposition onto Gold Surfaces by Scaling and Spectral Analysis of In Situ Atomic Force Microscopic Images," *J. Electrochem. Soc.*, vol. 143, no. 10, pp. 3122–3132, Oct. 1996.

[39] J. Goldstein, *Scanning electron microscopy and X-ray microanalysis*. New York [etc.]: Springer, 2003.

[40] "Instrumentation." [Online]. Available: http://www4.nau.edu/microanalysis/Microprobe-SEM/Instrumentation.html. [Accessed: 16-Jun-2013].

[41] D. B. Williams and C. B. Carter, *Transmission Electron Microscopy: A Textbook for Materials Science*. Springer, 2009.

[42] C. Srivastava, R.K. Rai, C. Srivastava, R.K. Rai, Transmission electron microscopy study of Ni-rich, Ag–Ni nanowires. Chem. Phys. Lett. 575, 91–96 (2013)..

[43] "SpringerImages - A schematic of a vibrating sample magnetometer. The sample is vibrated mechanically, and the induced signal in the sensing coils will be proportional to its magnetization." [Online]. Available: http://www.springerimages.com/Images/Geosciences/1-10.1007_978-1-4020-4423-6_204-2. [Accessed: 16-Jun-2013].

[44] Z. Peng and H. Yang, "Ag–Pt alloy nanoparticles with the compositions in the miscibility gap," *J. Solid State Chem.*, vol. 181, no. 7, pp. 1546–1551, Jul. 2008.

[45] E. C. Garnett, M. L. Brongersma, Y. Cui, and M. D. McGehee, "Nanowire Solar Cells," *Annu. Rev. Mater. Res.*, vol. 41, no. 1, pp. 269–295, 2011.

[46] R.K. Rai, C. Srivastava, R.K. Rai, C. Srivastava, Nonequilibrium microstructures for Ag–Ni nanowires. Microsc. Microanal. 21, 491–497 (2015).

[47] J. W. Edington, *Practical Electron Microscopy in Materials Science*. New York: Van Nostrand New York, 1976.

[48] U. Erb, A. M. El-Sherik, G. Palumbo, and K. T. Aust, "Synthesis, structure and properties of electroplated nanocrystalline materials," *Nanostructured Mater.*, vol. 2, no. 4, pp. 383–390, Jul. 1993.